Making a LIST and checking it twice:
Length scales of Instabilities and Stratified Turbulence

Colm-cille P. Caulfield[1,2], T. S. Eaves[2]

[1]BP Institute & [2]DAMTP, University of Cambridge
c.p.caulfield@bpi.cam.ac.uk

Abstract

Stratified shear flows, where the 'background' velocity and density distribution vary over some characteristic length scales, are ubiquitous in the atmosphere and the ocean. At sufficiently high Reynolds number, such flows are commonly believed to play a key role in the transition to turbulence, and hence to be central to irreversible mixing of the density field. Here, we review some of the recent progress in developing understanding of instability, transition, turbulence and mixing in stratified shear flows. In particular, we highlight certain non-intuitive aspects of the subtle interplay between the ostensibly stabilizing effect of stratification and destabilizing effect of velocity shear, especially when the density distribution has layers, i.e. relatively deep and well-mixed regions separated by relatively thin 'interfaces' of substantially enhanced density gradient.

1 Introduction

Stratified turbulent mixing is a key process in geophysically important flows in the atmosphere and ocean. Stratified mixing is enhanced by the presence of turbulent disordered motion, but understanding and modelling such turbulence has proved to be profoundly difficult. Indeed, the 'simpler' problem of turbulence in fluids of constant density may legitimately be described as **the** great unsolved problem in classical physics. For example, the classical 'inertial scaling' of the turbulent dissipation rate ϵ, defined as

$$\epsilon = 2\nu \left\langle s'_{ij} s'_{ij} \right\rangle; \ s'_{ij} = \frac{1}{2} \left(\frac{\partial u'_i}{\partial x_j} + \frac{\partial u'_j}{\partial x_i} \right); \mathbf{u} = \langle \mathbf{u} \rangle + \mathbf{u}', \tag{1}$$

is that $\epsilon \sim U^3/L$, where ν is the kinematic viscosity, the angled brackets are some appropriate spatial and/or temporal averaging, and U and L are some appropriate characteristic velocity scale and length scale. Comparing the scaling to the definition of ϵ, it is apparent that requiring the scaling in the limit as $\nu \to 0$ appears to imply a loss of smoothness in the symmetric part of the perturbation strain tensor s'_{ij}, the occurence of which is still an open (and million dollar) question.

The presence of a 'stable' stratification adds further, profound complication, even for the simplest possible class of model flows in the Boussineq, zero Mach number limit with a divergence-free velocity field and a linear equation of state, where the only dynamical effect of variations in fluid density relative to a hydrostatic base state is through the buoyancy force term in the vertical velocity equation. There are two obvious ways to appreciate this 'complication'. The first is that the presence of 'buoyancy' within the flow inevitably introduces anisotropy into the velocity components, with statically stable stratification tending to suppress vertical motions. The second is through consideration of the energetics of the flow. Since a key characteristic of turbulence is that the dissipation rate ϵ of 'turbulent' kinetic energy increases, there is thus an irreversible conversion of kinetic energy to internal energy, which within this simple class does not feed back on

the density field. When the fluid is stratified however, the potential energy of the flow can vary, and so now there are two possible ultimate sinks of the kinetic energy of the flow: irreversible loss to the internal energy reservoir and irreversible conversion to an increased potential energy of the system. Such irreversible conversion is associated with irreversible modification of the density of fluid parcels through molecular mixing, which it is enhanced significantly by turbulent motions.

Quantification of that mixing is central to parameterization of the vertical transport of heat in the ocean, a key part of the so-called 'meridional overturning circulation' (see for example Ferrari and Wunsch (2009)). Since mixing occurs on scales which are orders of magnitude too small to be captured by even regional models, idealised process studies are needed to identify and parameterize key processes. There has been a huge amount of research in this area, considering every stage of turbulent flow, from transition due to flow instability or boundary effects through the dynamics of quasi-stationary turbulence to ultimate late-time decay. It is becoming increasingly clear that any such parameterizations must capture a range of length scales of the flow. For example, during the stage of vigorous sheared turbulent motions in a stratified fluid, the dynamical behaviour varies qualitatively with the relative sizes of the Ozmidov length scale L_O, the Corrsin length scale L_C and the Kolmogorov length scale L_K defined as

$$L_O = \left(\frac{\epsilon}{N_b^3}\right)^{1/2}, \; L_C = \left(\frac{\epsilon}{S_b^3}\right)^{1/2}, \; L_K = \left(\frac{\nu^3}{\epsilon}\right)^{1/4}, \tag{2}$$

where N_b and S_b are some appropriate outer scale buoyancy frequency, and velocity shear respectively. The so-called buoyancy Reynolds number Re_B, which is commonly used as a measure of the intensity of turbulence in a stratified fluid is defined as

$$Re_B = \frac{\epsilon}{\nu N_b^2} = \left(\frac{L_O}{L_K}\right)^{4/3}, \tag{3}$$

Therefore, flow regimes, characteristic of the oceans where $Re_B \gg 1$ (see for example Brethouwer et al. (2007)) are associated with a large scale separation between L_O and L_K, thus allowing for the existence of a classical inertial range of scales much larger than the Kolmogorov scale (and so unaffected by viscosity) and much smaller than the Ozmidov scale (and so not strongly affected by the stratification).

Of course, these are by no means the only dynamically important length scales. Indeed, it is becoming increasingly apparent that much of the world's oceans are in a strongly stratified turbulent regime, characterised by very small **horizontal** Froude number F_h yet order one **vertical** Froude number F_v, defined as

$$F_h = \frac{U}{N_b L_h} \ll 1, \; F_v = \frac{U}{N_b L_v} \sim O(1), \tag{4}$$

where L_h and L_v are some characteristic horizontal and vertical scales. As shown by Billant & Chomaz and Lindborg (see Brethouwer et al. (2007) for discussion), the ordered scaling $L_v \gg L_h \gg L_O \gg L_K$ leads to an inherently stratified turbulence regime with significant anisotropy in the velocity components (with $w \ll u, v$) and yet a forward cascade with a horizontal energy spectrum exhibiting a $k^{-5/3}$ power law dependence on the horizontal wavenumber k.

2 Layered flows

Importantly, this regime implies that such stratified turbulent flow is generically layered, in that the flow arranges itself in such a way that characteristic horizontal scales are much larger than characteristic vertical scales. There is increasing observational evidence (Falder et al. (2016)) of such 'layered anisotropic stratified turbulence' (LAST) occuring in the ocean, and so there is a natural need to consider the behaviour of 'layered' stratified flows, where 'layers' of relatively deep regions of relatively weakly stratified fluid are separated by 'interfaces', relatively shallow regions of relatively strongly stratified fluid. Of course, it is not just LAST that can lead to layered density distributions. It is well-known that double diffusive processes produce characteristic, and commonly observed staircases. Furthermore, as originally proposed by Phillips (1972), if the vertical buoyancy flux varies non-monotonically with overall stratification, the development of layer/interface structure in the density field is inevitable. Such a structure has been observed in reduced models (Balmforth et al. (1998)) and experiments (Oglethorpe et al. (2013)), though it is an open, and important question whether this non-monotonicity is generic of stratified mixing.

Layered stratified shear flows have very different stability properties from flows with more uniformly varying density, as in the presence of a large-scale shear, such flows have non-trivial structure in the gradient Richardson number $Ri_g(y,t) = N_b^2/S_b^2$, Such non-trivial structure generically ensures that the classic Miles-Howard criterion does not apply, even when the overall stratification is very 'strong', and so flow instabilities are not typically precluded. Just such a layered stratified shear flow was considered originally by Taylor in his famous Adams Prize essay of 1915 on 'Turbulent motions in fluids', in which he also derived the Taylor-Goldstein equation for the linear stability properties of an inviscid stratified shear flow. This equation was actually only published in Taylor (1931), and Taylor explained the delay because he was unable to '*undertake experiments designed to verify, or otherwise, the results*' of the instability of a multi-layered stratified shear flow whose existence he predicted. This 'Taylor' instability has received relatively little attention, certainly compared to the classic overturning Kelvin-Helmholtz instability (KHI) of inflectional shear layers or even the Holmboe wave instability (HWI)which appears when a relatively sharp density interface is embedded in a shear layer.

The growth mechanisms of these instabilities can be explained short-wave is in terms of 'wave interaction theory' (WIT) as reviewed in Carpenter et al. (2011). The KHI arises due to the Doppler-shifted interaction between vorticity waves which arise at the two edges of the shear layer, while the HWI arises due to the interaction between one of the vorticity waves and an internal wave localized on the relatively sharp density interface. Both of these instabilities are commonly observed in nature, experiments and numerical simulations. They are known to be prone to a 'zoo' of secondary instabilities which trigger the ultimate transition to turbulence and are thought to be key drivers of mixing, and indeed layer formation and maintenance (Mashayek et al. (2013); Salehipour et al. (2016)). However, much less is known about the instability originally considered by Taylor. It is qualitatively different, as it does not rely upon the existence of a finite depth shear layer or an inflectional velocity profile. It occurs (in its simplest form) in a three-layer, two interface stratified fluid with a constant shear across the entire layer, and arises due to the Doppler-shifted interaction between two internal waves on each of the two density interfaces. It is an inherently stratified instability, and clearly demonstrates that static stability can actually **destabilize** stratified shear flows. Recently, there has been some renewed interest in the linear stability properties of this instability (Carpenter et al.

(2010); Guha and Lawrence (2014); Heifetz and Mak (2015); Churilov (2016)) but study of its finite amplitude behaviour has been strangely neglected (Caulfield et al. (1995); Lee and Caulfield (2001); Balmforth et al. (2012)).

The instability appears to rely on interfaces being relatively 'sharp', which presents computational challenges that are only recently being addressed. As discussed above however, there are many reasons why stratified turbulent flows may naturally form 'sharp' interfaces, and so it is of real geophysical interest to investigate the properties of such flows. There has been some recent evidence in a reduced, effectively long-wave model discussed in Balmforth et al. (2012) that this Taylor instability also differs qualitatively in character from the KHI and HWI, in that there is a suggestion that it is very 'fragile', and rapidly breaks down, even in two dimensions. This breakdown appears to non-trivially modify the mean flows to encourage the appearance of secondary HWI, which are themselves much more robust and long-lived. This picture is consistent with the apparent difficulties which Taylor found in observing this instability experimentally. Here, we discuss some numerical simulations of two-dimensional flow at relatively high Reynolds number and Prandtl number $Pr = \nu/\kappa$ (κ is the density diffusivity) which investigate the nonlinear evolution and robustness of this instability.

3 Results

3.1 Flow geometry

We consider a two-dimensional three-layer Boussinesq fluid in a plane Couette flow (PCF) geometry. The two channel walls of the PCF are moving at speeds $\pm \Delta U$, and the fluid at $\pm h$ has fixed density of $\rho_0 \mp \Delta \rho$. The Reynolds number Re, Prandtl number Pr and bulk Richardson number Ri_B are given by

$$Re = \frac{\Delta U h}{\nu}, \quad Pr = \frac{\nu}{\kappa}, \quad Ri_B = \frac{g \Delta \rho h}{\rho_0 \Delta U^2}. \tag{5}$$

In figure 1 we plot the nondimensional streamwise base velocity distribution $U(y)$ and the initial base density distribution $\bar{\rho}(y) - \rho_0/\Delta \rho$ for $R = 20$ and $R \to \infty$, where

$$\boldsymbol{U}(y) = U(y)\boldsymbol{x} = y\hat{\boldsymbol{x}}, \quad \bar{\rho}(y) - \frac{\rho_0}{\Delta \rho} = -\frac{1}{2} \left[\tanh R(y - 1/3) + \tanh R(y + 1/3) \right]. \tag{6}$$

The gradient Richardson number $Ri_g(y)$ for the base flow defined by (6) is

$$Ri_g(y) \equiv -Ri_B \frac{\frac{\partial \rho_{tot}}{\partial y}}{\left(\frac{\partial u_{tot}}{\partial y} \right)^2} = \frac{Ri_B R}{2} \left[\text{sech}^2 R(y - 1/3) + \text{sech}^2 R(y + 1/3) \right] \tag{7}$$

which is very close to zero for a large range of y for all bulk Richardson numbers Ri_B. Specifically, there are broad regions of the flow for which $Ri(y) < 1/4$, and so there is at least the possibility of linear instability for all values of Ri_B.

3.2 Linear stability properties

We consider this particular flow for two technical reasons. First, unstratified PCF is linearly stable for all Reynolds numbers and so any instability in this particular flow demonstrates the destabilizing effect of static instability. Second, there is no finite depth
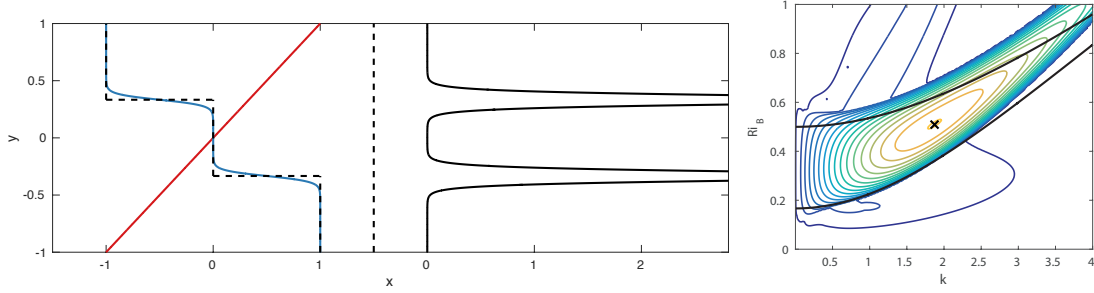
Figure 1: a) Vertical variation of base flow velocity $U(y)$ (red), base flow density distribution $\bar{\rho}(z) - \rho_0/\Delta\rho$ with $R = 20$ (blue) and $R \to \infty$ (dashed line) as defined in (6). b) Vertical variation of gradient Richardson number $Ri_g(y)$ as defined in (7) for the base flow density distribution with $R = 20$ shown in a). The maximum value $Ri_g(\pm 1/3) = 5.22$. c) Contours of the largest modal growth rate σ for $Re = 5000$, $Pr = 70$ and $R = 20$. The outermost (and darkest) blue contour has $\sigma = 0$, and there is a constant contour interval of 0.005. The cross marks the values of wavenumber and Ri_B which are numerically simulated: $\alpha = 1.87$, $Ri_B = 0.51$, with growth rate $\sigma = 0.093$. The black solid lines show the stability boundary for the piecewise linear density profile shown with a dashed line in panel a).

shear layer, and so a primary KHI is precluded. Therefore, any observed instability must be of the type considered by Taylor. Indeed, a conventional analysis of the stratified Orr-Somerfeld equation shows that this flow is linearly unstable for arbitrary Ri_B as shown in figure 1c. We assume perturbations of normal mode form: $(\boldsymbol{u}, \rho) = [\hat{\boldsymbol{u}}(y), \hat{\rho}(y)] \exp(ik[x - ct])$ and $\sigma = kc_i$. Contours of growth rate σ are plotted in figure 1c. The black solid lines show the marginal contours for the stability of an inviscid flow with stepwise density distribution as shown with the dashed black lines in figure 1a, which has a very similar structure to the band of instability first determined by TaylorTaylor (1931), and so it is clearly appropriate to identify this branch of instability (with zero real phase speed) as being of the same kind.

3.3 Nonlinear dynamics

We study the two-dimensional, nonlinear evolution of both primary and secondary instabilities in a flow corresponding to the parameters marked with a cross in figure 1c, i.e. $Re = 5000$, $Pr = 70$, $Ri_B = 0.51$ and $L_x = 6.72$, corresponding to two wavelengths of the most unstable mode of linear theory. The equations of motion were integrated using Diablo, a parallel Fortran-based Navier–Stokes time-stepping numerical pseudo-spectral code developed by T. Bewley and J. R. Taylor at UCSD. We use a 2048×2033 grid, which is more than sufficient to capture the dynamics. We initialise the simulations with a small amplitude of the unstable modal form and a smaller amplitude solenoidal noise field to allow for secondary instabilities. The noise accounts for 1% by amplitude of the initial condition perturbation. Figure 2 shows snapshots of the flow at different points during the evolution of the system. The primary instability results in cusps and streaks of vorticity forming on the density interfaces, pulling them towards each other as can be seen in the first panel of figure 2. These vorticity streaks then begin to roll up to form two coherent vortical cores, as the finite amplitude manifestation of this instability. These vortical cores begin to lose energy as they are sheared out, and there is a misalignment of the cusps on the density interfaces, resulting in the creation of two more vortical cores located between the primary pair of vortical cores as is evident in the second panel of figure 2. The two newly created vortical cores begin to grow in size and appear to squeeze
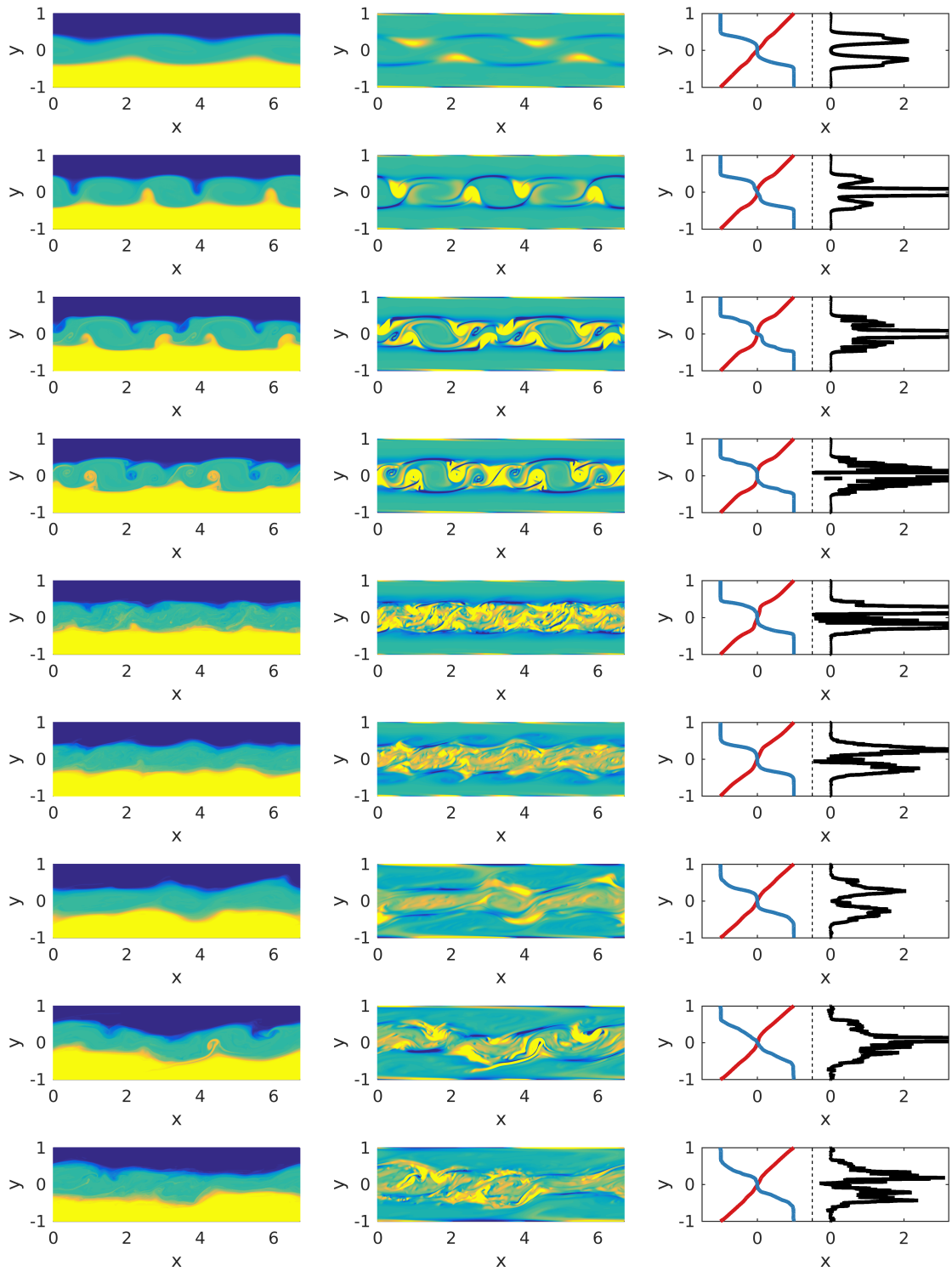
Figure 2: Snapshots of the nonlinear flow evolution at various times. Left hand column shows total density field, middle column shows perturbation vorticity field and right hand column shows the mean horizontal velocity (red), mean density (blue) and notional associated gradient Richardson number (black) at $t = 70, 95, 100, 125, 140, 200, 380$ and 400.

the two original vortical cores. This causes complex spatio-temporal vorticity dynamics within the two original vortical cores, as is evident in the third and fourth panels of figure 2. The squeezing of the two original vortical cores causes a cascade of secondary braid-like instabilities that results in small-scale disorder in the intermediate layer, and a destruction of the cusps on the two density interfaces due to vigorous mixing in the intermediate layer. The disordered vorticity field is evident in the fifth panel of figure 2.

The mean velocity profile during this disordered state exhibits increased shear over the laminar profile at each of the two density interfaces. This increased shear spontaneously creates eight regions of negative vorticity, four above the upper density interface and four below the lower density interface, as seen in the sixth panel of figure 2. These vortices also cause wisps of fluid from the intermediate density layer into both the upper and lower density layers, and are due to the parasitic secondary appearance of a nonlinear Holmboe wave, associated with the localized intensified shear in the vicinity of each density interface. The vigorous mixing associated with the braid-instability-driven decay of the evolution of the primary instability has rearranged the mean fields in just such a way to cause the flow to become susceptible to the appearance of HWI. Soon after the appearance of wavelength four nonlinear Holmboe waves there is a coarsening to wavelength two nonlinear Holmboe waves, as is apparent from the two vortices above the upper density interface and two vortices below the lower density interface in the seventh panel in figure 2. The wavelength two nonlinear Holmboe wave state gradually increases in energy during $150 \lesssim t \lesssim 275$. The peak in energy at $t \approx 275$ appears to correspond with the wavelength two state interacting with the flow boundaries, and this mediates the end of continued energy growth. As the flow begins to decay, there is yet another coarsening event, and the flow settles onto a large amplitude single wavelength nonlinear Holmboe wave for $t \gtrsim 350$. This final state, which is visible in the bottom two panels of figure 2, is reminiscent of the large amplitude nonlinear Holmboe wave found by Balmforth et al. (2012).

4 Conclusions

Although such two-dimensional simulations at high Reynolds number should be treated with caution, two key conclusions consistent with the results of Balmforth et al. (2012) can be drawn. First, the Taylor instability is clearly 'fragile' and prone to strong secondary two-dimensional instabilities at high Reynolds number. Second, those secondary instabilities can modify the base flow in a way that then leads to the 'parasitic' development of HWI at later times in layered stratified shear flows. This is apparently due to the local intensification of shear at each of the relatively sharp density interfaces, as is apparent in the fifth panel of figure 2. Therefore, we may conclude that the instability first described by Taylor can grow very strongly in layered stratified shear flows, which as we have argued are likely to be very common in geophysical flows prone to vigorous stratified turbulence. This instability however appears to be extremely fragile to secondary instabilities, even in two dimensions, and so it is unsurprising that it has proved difficult to observe. That does not mean it is unimportant however, as it can strongly modify the mean flow in such a way to trigger Holmboe instabilities, which appear to be very robust. To 'close the loop' of relevance to real geophysical flows however, it is clearly important to consider the mixing properties of such flows in three dimensions, to investigate in particular whether they differ strongly from other more widely studied flows, such as flows prone to primary overturning instabilities of Kelvin-Helmholtz type.

References

Balmforth, N. J., Llewellyn Smith, S. G., and Young, W. R. (1998). Dynamics of interfaces and layers in a stratified turbulent fluid. *J. Fluid Mech.*, 355:329–358.

Balmforth, N. J., Roy, A., and Caulfield, C. P. (2012). Dynamics of vorticity defects in stratified shear flow. *J. Fluid Mech.*, 694:292–331.

Brethouwer, G., Billant, P., Lindborg, E., and Chomaz, J.-M. (2007). Scaling analysis and simulation of strongly stratified turbulent flows. *J. Fluid Mech.*, 585:343–368.

Carpenter, J. R., Balmforth, N. J., and Lawrence, G. A. (2010). Identifying unstable modes in stratified shear layers. *Phys. Fluids*, 22:054104.

Carpenter, J. R., Tedford, E. W., Heifetz, E., and Lawrence, G. A. (2011). Instability in stratified shear flow: Review of a physical interpretation based on interacting waves. *Appl. Mech. Rev.*, 64:060801.

Caulfield, C. P., Peltier, W. R., Yoshida, S., and Ohtani, M. (1995). An experimental investigation of the instability of a shear flow with multilayered density stratification. *Phys. Fluids*, 7:3028.

Churilov, S. M. (2016). Stability of shear flows with multilayered density stratification and monotonic velocity profiles having no inflection points. *Geophys. Astrophys. Fluid Dyn.*, 110:78–108.

Falder, M., White, N. J., and Caulfield, C. P. (2016). Seismic imaging of rapid onset of stratified turbulence in the south Atlantic Ocean. *J. Phys. Oceanogr.*, 46:1023–1044.

Ferrari, R. and Wunsch, C. (2009). Ocean circulation kinetic energy: Reservoirs, sources and sinks. *Annu. Rev. Fluid Mech.*, 41:253–282.

Guha, A. and Lawrence, G. A. (2014). A wave interaction approach to studying non-modal homogeneous and stratified shear instabilities. *J. Fluid Mech.*, 755:336–364.

Heifetz, E. and Mak, J. (2015). Stratified shear flow instabilities in the non-Boussinesq regime. *Phys. Fluids*, 27:086601.

Lee, V. and Caulfield, C. P. (2001). Nonlinear evolution of a layered stratified shear flow. *Dyn. Atmos. Ocean.*, 34:103–124.

Mashayek, A., Caulfield, C. P., and Peltier, W. R. (2013). Time-dependent, non-monotonic mixing in stratified turbulent shear flows: implications for oceanographic estimates of buoyancy flux. *J. Fluid Mech.*, 736:570–593.

Oglethorpe, R. L. F., Caulfield, C. P., and Woods, A. W. (2013). Spontaneous layering in stratified turbulent Taylor–Couette flow. *J. Fluid Mech.*, 721:R3.

Phillips, O. M. (1972). Turbulence in a strongly stratified fluid - is it unstable? *Deep-Sea Res.*, 19:79–81.

Salehipour, H., Caulfield, C. P., and Peltier, W. R. (2016). Turbulent mixing due to the Holmboe wave instability at high Reynolds number. *J. Fluid. Mech.*, XXX:in proof.

Taylor, G. I. (1931). Effect of variation in density on the stability of superposed streams of fluid. *Proc. R. Soc. Lond.*, 132:449–523.